

An idealised description of the frictional receding contact behaviour of a bolted joint

J.P. Lopes^{a,*}, D.A. Hills^a

^a*Department of Engineering Science, University of Oxford,
Parks Road, Oxford OX1 3PJ, United Kingdom*

Abstract

This paper proposes a description for the contact behaviour of bolted joints through the solution of the frictional axisymmetric receding contact of a semi-infinite layer pressed against an elastically similar half-space by uniform pressure over a disk of radius b . First, the contact is assumed to be adhered and closed, and a bilateral solution is obtained. The adhered solution is then corrected using an integral formulation based on a kernel of circular dislocation loop to describe the interfacial tractions at the regions where partial slip and opening occur. A numerical solution is obtained for the corrected tractions and radius of slip and opening.

Keywords: Axisymmetric, Receding Contact, Ring dislocations, Bolted joints

1. Introduction

One of the ways to classify contacts is to observe whether or not new points come in contact as the bodies deform. In receding contacts, the application of a normal load causes a reduction in the size of the contact. A property of some receding contacts is that the contact area in the deformed configuration is independent of the applied load and, consequently, the change between undeformed/deformed configurations is discontinuous, i.e. the contact ‘snaps’ to the deformed configuration upon applying a normal load [1]. This presents a challenge in obtaining solutions through the Finite Element Method, as a large portion of the nodes change status from being in contact to being free when an infinitesimal normal load is applied.

Amongst the examples of axisymmetric receding contacts is the contact in bolted joints. Even though this type of fixing is ubiquitous in industry, the description of axisymmetric receding contacts in the literature is still restricted to either plane problems [2, 3] or frictionless cases [4, 5, 6]. More recently, a solution for an axisymmetric receding contact of a layer pressed against a half-space by a point load has been presented [7]. Even though the fundamental nature of this solution is crucial to better understanding receding contacts, in reality the bolt load is spread over a washer which distributes pressure over a finite disk.

In order to model better the normal characteristics of a bolted joint, the effect of the bolt/washer loading over the layer will be modelled by a disk of pressure. This paper proposes, then, the study of the frictional axisymmetric receding contact of a homogeneous semi-infinite layer of

thickness a , Poisson’s ratio ν and modulus of rigidity μ , pressed against an elastically similar half-space $z \geq a$ (Figure 1a) by a disk of pressure applied to the layer’s surface ($z = 0$), such that

$$\sigma_{zz}(r, 0) = -p, \quad 0 \leq r \leq b \quad (1)$$

$$\sigma_{zz}(r, 0) = 0, \quad r > b. \quad (2)$$

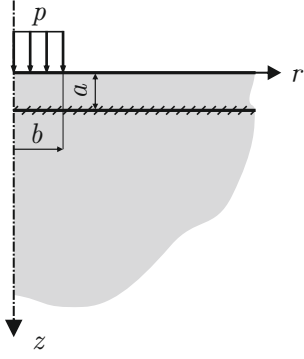
Furthermore, the objective of this study is to find the solution to the proposed problem using ring dislocations to introduce corrections to the stresses in the contact interface as a distribution of strain nuclei. First, we assume that the contact is in a fully closed and stuck configuration. We then apply dislocation densities to correct the stresses when this condition is violated. This methodology has been presented in previous papers by the authors [8, 7].

2. Adhered Solution

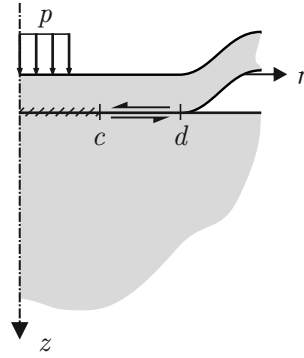
We start our analysis by assuming that the applied pressure induces normal and shear tractions at the layer/half-space interface such that the contact remains closed and stuck throughout this region, i.e. the contact pressure is compressive everywhere and the shear traction is limited by Coulomb friction. Following this assumption, the state of stress in the bodies is equivalent to an augmented half-space $z \geq 0$ under the same loading (Figure 1a). In the cylindrical coordinate set shown in the figure, the state of stress is given by Love [9, 10, 11] and the tractions $\tilde{\sigma}_{ij}(r, z)$ arising on any radial plane ($z = \text{constant}$ surface) are given by:

*Corresponding author

Email addresses: jhonatan.dapontelopes@eng.ox.ac.uk (J.P. Lopes), david.hills@eng.ox.ac.uk (D.A. Hills)



(a)



(b)

Figure 1: A layer subjected to semi-infinite pressure. (a) Fully closed and stuck. (b) Partially open and slipping.

$$\tilde{\sigma}_{zz}(r, z) = p \left\{ \frac{2z}{\pi} \left[\frac{r^2 + z^2 - b^2}{(l_2)^3 (1 - k^2)^2} \mathbf{E}(k) + \frac{b^2 - (l_1)^2}{(l_2)^3 (1 - k^2)} \mathbf{K}(k) - \frac{1}{l_2} \mathbf{\Pi}(n; k) \right] \right\} \quad (3)$$

$$\tilde{\sigma}_{rz}(r, z) = -p \left\{ \frac{2z^2}{\pi} \left[\frac{(1 + k^2) \mathbf{E}(k) - (1 - k^2) \mathbf{K}(k)}{(k^2 - 1)^2 l_2 r} \right] \right\} \quad (4)$$

where

$$l_1 = \frac{1}{2} \left\{ \sqrt{(r + b)^2 + z^2} - \sqrt{(r - b)^2 + z^2} \right\} \quad (5)$$

$$l_2 = \frac{1}{2} \left\{ \sqrt{(r + b)^2 + z^2} + \sqrt{(r - b)^2 + z^2} \right\} \quad (6)$$

$$k = \frac{l_1}{l_2} \quad (7)$$

$$n = \left(\frac{l_1}{r} \right)^2 \quad (8)$$

and $\mathbf{K}(k)$, $\mathbf{E}(k)$, $\mathbf{\Pi}(n; k)$ are the complete elliptic integrals of the first, second and third kind respectively. These func-

tions are continuous and bounded at every point inside the half-space, but $\mathbf{\Pi}(n; k)$ cannot be evaluated numerically along the z -axis, since $r = 0$ there. In this region, we take the limits as $r \rightarrow 0$, giving:

$$\tilde{\sigma}_{zz}(0, z) = -p \left\{ \frac{z^3}{(b^2 + z^2)^{3/2}} \right\} \quad (9)$$

$$\tilde{\sigma}_{rz}(0, z) = 0. \quad (10)$$

When $b \rightarrow 0$ and $p \rightarrow \infty$, we would expect the bilateral loading due to the circular patch of pressure (eqs. (3) and (4)) to converge to the stress distribution due to a concentrated point force applied at the origin [7]. However, taking the limits results in:

$$\lim_{b \rightarrow 0} \tilde{\sigma}_{zz}(r, z) = 0 \quad (11)$$

$$\lim_{b \rightarrow 0} \tilde{\sigma}_{rz}(r, z) = 0. \quad (12)$$

Therefore, even if the pressure is infinite, the limiting stress distribution would be a constant over the half-space. Hence, the circular patch of pressure and the point force are inherently different loadings and result in distinct stress distributions even in the limiting case where $b \rightarrow 0$.

If the contact is, indeed, fully closed and adhered, the normal $N(r)$ and shear $S(r)$ tractions at the layer/half-space interface are given by:

$$N(r) = \tilde{\sigma}_{zz}(r, a) \quad (13)$$

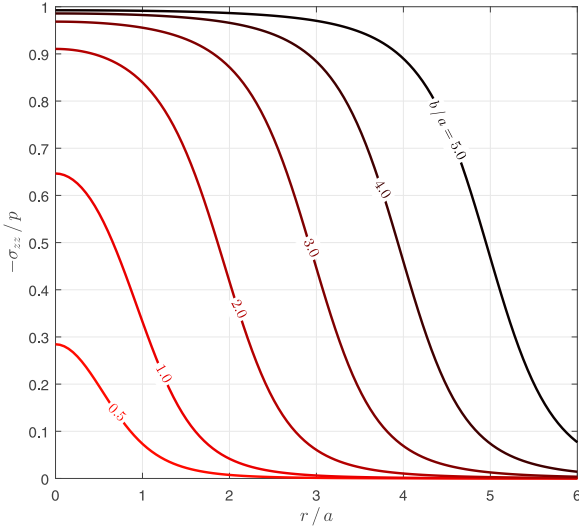
$$S(r) = \tilde{\sigma}_{rz}(r, a). \quad (14)$$

Figure 2 shows the normalised contact pressure and shear to normal stress ratio for the adhered solution. Analysing the stress ratio (Figure 2b), we notice that no realistic value of coefficient of friction would be high enough to prevent slip as $r/a \rightarrow \infty$. Furthermore, for all values of b/a the contact pressure (Figure 2a) eventually falls to zero at the contact interface, which results in the development of an open region.

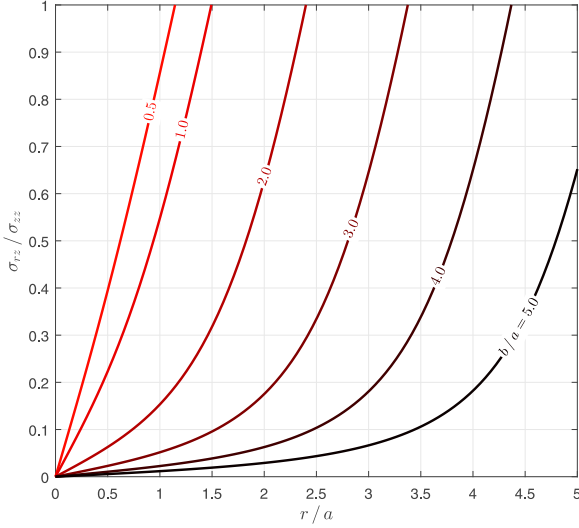
3. Formulation

The bilateral solution developed in Section 2 is, therefore, not valid, as the assumption that the contact is fully stuck and closed is violated for realistic values of f and b/a . The contact should develop regions where it is closed and partially slipping and regions where it is open, as shown in Figure 1b.

It is necessary to correct the bilateral solution in order to satisfy opening and slipping conditions. A modified solution can be developed by representing the tractions at the contact interface as a sum of the bilateral (adhered) solution with a correction in the form of an integral representation of slip and opening as a distribution of glide and



(a)



(b)

Figure 2: Normalised tractions for the adhered (bilateral) solution. (a) Normalised contact pressure. (b) Shear to normal stress ratio.

climb dislocations, respectively. The dislocations needed are all of ‘edge’ type, with their Burger’s vectors resting in a $\theta = \text{constant}$ plane. We stress that the insertion of dislocations is used only as a mathematical device to correct the tractions in our formulation as a distribution of strain nuclei. This does not mean that physical defects are being inserted in the micro-structure of the material. Detailed explanations of the method can be found in [12, 7, 8].

In order to model contact slip, we introduce a radial $b_r(\xi)$ glide dislocation loop of radius ξ , placed at a depth a . It may be created by cutting a path along the annular disk $\xi \leq r \leq \infty$ and sliding the surfaces by a constant amount b_r . This will introduce the following tractions along the

path cut disk

$$\hat{\sigma}_{iz}(r) = G_{iz}^r(r, \xi) b_r(\xi). \quad (15)$$

The influence functions $G_{iz}^r(r, \xi)$ are described as sums of Lipschitz-Hankel integrals and have extremely complicated forms. For a half-space, these are given by Paynter et al. [13] (see also [14, 15]) and in the Appendix A. They are bounded (‘regular’) when $i = z$ and display a Cauchy singularity when $i = r$.

The modelling of contact opening is done by introducing an axial $b_z(\xi)$ climb dislocation loop of radius ξ , lying at a depth a . Now, the dislocation loop may be formed by making a path cut along $\xi \leq r \leq \infty$ and inserting a disk of thickness b_z . This will induce the following tractions $\hat{\sigma}_{iz}(r)$ ($i = r, z$) along the path cut disk

$$\hat{\sigma}_{iz}(r) = G_{iz}^z(r, \xi) b_z(\xi). \quad (16)$$

Once again, the influence functions $G_{iz}^z(r, \xi)$ are functions of Lipschitz-Hankel integrals. For a half-space, these are also given by Paynter et al. [13]. This time, they are bounded (‘regular’) when $i = r$ and display a Cauchy singularity when $i = z$.

From the bilateral solution, we expect the contact to be closed and stuck from the origin to a radius $r = c$, closed and slipping in the region $c \leq r \leq d$, and open in a region extending from a radius d to infinity. Both the closure point d and stick point c are outputs of the problem (self-determining points).

The resulting normal $N(r)$ and shear $S(r)$ tractions along the contact interface are given by

$$N(r) = \tilde{\sigma}_{zz}(r) + \int_d^\infty G_{zz}^z(r, \xi) B_z(\xi) d\xi + \int_c^\infty G_{zz}^r(r, \xi) B_r(\xi) d\xi, \quad (17)$$

$$S(r) = \tilde{\sigma}_{rz}(r) + \int_d^\infty G_{rz}^z(r, \xi) B_z(\xi) d\xi + \int_c^\infty G_{rz}^r(r, \xi) B_r(\xi) d\xi, \quad (18)$$

where $B_i(\xi) = db_i/d\xi$, $i = r, z$ represents the dislocation density. Glide dislocations are installed over the whole of the length of the contact interface where slipping occurs, including the open portion, and climb dislocations are installed over the part of the contact interface which is open. Equations (17) and (18) form the basis of the solution and integral equations may be generated to restore conventional Signorini inequalities.

In the open region, we require the surfaces to be traction-free

$$N(r) = 0, \quad S(r) = 0, \quad d \leq r \leq \infty \quad (19)$$

whereas, in the closed, slipping region, the shearing traction is limited by friction:

$$N(r) < 0 \quad S(r) = f N(r) \quad c \leq r \leq d. \quad (20)$$

The three sets of conditions in eqs. (19) and (20) may be combined into two by making use of the Heaviside step function, $H(\cdot)$, giving

$$N(r) = 0 \quad d \leq r \leq \infty \quad (21)$$

$$S(r) - f H(d - r) N(r) = 0 \quad c \leq r \leq \infty. \quad (22)$$

Applying eqs. (17) and (18) to eqs. (21) and (22), gives

$$\int_c^\infty G_{zz}^r(r, \xi) B_r(\xi) d\xi + \int_d^\infty G_{zz}^z(r, \xi) B_z(\xi) d\xi = -\tilde{\sigma}_{zz}(r) \quad d \leq r \leq \infty \quad (23)$$

$$\int_c^\infty \left[G_{rz}^r(r, \xi) - f H(d - r) G_{zz}^r(r, \xi) \right] B_r(\xi) d\xi + \int_d^\infty \left[G_{rz}^z(r, \xi) - f H(d - r) G_{zz}^z(r, \xi) \right] B_z(\xi) d\xi = -\left[\tilde{\sigma}_{rz}(r) - f H(d - r) \tilde{\sigma}_{zz}(r) \right] \quad c \leq r \leq \infty. \quad (24)$$

Due to the nature of the functions present in eqs. (23) and (24), there is no expectation of obtaining an analytical inversion of the integral equations. We must solve the singular integral equations numerically, choosing to use Gauss-Chebyshev quadrature [16]. Since there are two regions of imposition for the integral equations, two sets of quadrature points are needed. Notice that in eq. (23), the kernel $G_{zz}^r(r, \xi)$ is Cauchy singular over the region $d \leq r, \xi \leq \infty$ while $G_{zz}^z(r, \xi)$ is regular. In eq. (24), the kernel $G_{rz}^r(r, \xi)$ is Cauchy singular over the region $c \leq r, \xi \leq \infty$ while all the other terms are regular. Since there is no overlap of Cauchy regions, the two sets of quadrature are sufficient and no special interpolation is needed.

The first step in solving the SIEs is to put the integrals in standard form over the interval $[-1, 1]$. The following transformation functions were proposed to map a normalised coordinate t to a physical coordinate r :

$$r = \frac{\lambda(t+1) + 2\hat{r}}{1-t} \quad (25)$$

$$r = \hat{r} + \lambda \log\left(\frac{2}{1-t}\right) \quad (26)$$

$$r = \hat{r} \left[1 + \lambda \tanh^{-1}\left(\frac{2}{1-t}\right) \right], \quad (27)$$

where \hat{r} corresponds to the lower bound of the physical interval $[\hat{r}, \infty]$ and λ is a scaling parameter.

From the proposed mappings, the logarithm transformation resulted in the best description of the solution as

well as the best convergence. Hence, normalising the integrals using the following substitutions:

$$u = 1 - 2 \exp\left(\frac{d-\xi}{\lambda}\right), \quad d \leq \xi \leq \infty \quad (28)$$

$$v = 1 - 2 \exp\left(\frac{d-r}{\lambda}\right), \quad d \leq r \leq \infty \quad (29)$$

$$s = 1 - 2 \exp\left(\frac{c-\xi}{\lambda}\right), \quad c \leq \xi \leq \infty \quad (30)$$

$$t = 1 - 2 \exp\left(\frac{c-r}{\lambda}\right), \quad c \leq r \leq \infty. \quad (31)$$

gives

$$\int_{-1}^1 G_{zz}^r(v, s) B_r(s) \left(\frac{d\xi}{ds}\right) ds + \int_{-1}^1 G_{zz}^z(v, u) B_z(u) \left(\frac{d\xi}{du}\right) du = -\tilde{\sigma}_{zz}(v) \quad -1 \leq v \leq 1 \quad (32)$$

$$\int_{-1}^1 B_r(s) \left[G_{rz}^r(t, s) + f H(\gamma) G_{zz}^r(t, s) \right] \left(\frac{d\xi}{ds}\right) ds + \int_{-1}^1 B_z(u) \left[G_{rz}^z(t, u) + f H(\gamma) G_{zz}^z(t, u) \right] \left(\frac{d\xi}{du}\right) du = -\left[\tilde{\sigma}_{rz}(t) + f H(\gamma) \tilde{\sigma}_{zz}(t) \right] \quad -1 \leq t \leq 1 \quad (33)$$

where

$$\gamma = 1 - \frac{c}{d} + \frac{\lambda}{d} \log\left(\frac{1-t}{2}\right) \quad (34)$$

$$\frac{d\xi}{ds} = \frac{\lambda}{1-s} \quad (35)$$

$$\frac{d\xi}{du} = \frac{\lambda}{1-u}. \quad (36)$$

For the general form of the solution, both the climb and glide dislocations must be bounded at both ends of the interval. Thus, we choose

$$B_r(s) = \phi_r(s) \sqrt{1-s^2} \quad (37)$$

$$B_z(u) = \phi_z(u) \sqrt{1-u^2} \quad (38)$$

and eqs. (32) and (33) become, in normalised form,

$$\begin{aligned}
& \sum_{i=1}^N \left\{ \frac{\lambda W_i}{1-s_i} \phi_r(s_i) G_{zz}^r(v_k, s_i) \right\} + \\
& \sum_{i=1}^N \left\{ \frac{\lambda X_i}{1-u_i} \phi_z(u_i) G_{zz}^z(v_k, u_i) \right\} \\
& = -\frac{2}{\pi} \tilde{\sigma}_{zz}(v_k) \quad k = 1, \dots, N+1
\end{aligned} \tag{39}$$

$$\begin{aligned}
& \sum_{i=1}^N \left\{ \left[G_{rz}^r(t_k, s_i) - f H(\gamma_k) G_{zz}^r(t_k, s_i) \right] \frac{\lambda W_i}{1-s_i} \phi_r(s_i) \right\} + \\
& \sum_{i=1}^N \left\{ \left[G_{rz}^z(t_k, u_i) - f H(\gamma_k) G_{zz}^z(t_k, u_i) \right] \frac{\lambda X_i}{1-u_i} \phi_z(u_i) \right\} \\
& = -\frac{2}{\pi} \left[\tilde{\sigma}_{rz}(t_k) - f H(\gamma_k) \tilde{\sigma}_{zz}(t_k) \right] \quad k = 1, \dots, N+1
\end{aligned} \tag{40}$$

where

$$\gamma_k = 1 - \frac{c}{d} + \frac{\lambda}{d} \log \left(\frac{1-t_k}{2} \right) \tag{41}$$

and the integration points s_i, u_i , collocation points t_k, v_k and weights W_i, X_i for the quadrature are given as [16]

$$s_i = u_i = \cos \left(\pi \frac{i}{N+1} \right) \quad i = 1, \dots, N \tag{42}$$

$$t_k = v_k = \cos \left(\frac{\pi}{2} \frac{2k-1}{N+1} \right) \quad k = 1, \dots, N+1 \tag{43}$$

$$W_i = X_i = \frac{1-s_i^2}{2(N+1)}. \tag{44}$$

Equations (39) and (40) form a system of $2N+2$ equations and $2N+2$ unknowns. These are the N values of $\phi_r(s_i)$, N values of $\phi_z(u_i)$, the closure point d and the stick point c . Once ϕ_r and ϕ_z are known, the stresses at a point (r, z) can be found by the discrete versions of eqs. (17) and (18)

$$\begin{aligned}
N(v) = & \tilde{\sigma}_{zz}(v) + \sum_{i=1}^N \left\{ \frac{\lambda W_i}{1-s_i} \phi_r(s_i) G_{zz}^r(v, s_i) \right\} + \\
& \sum_{i=1}^N \left\{ \frac{\lambda X_i}{1-u_i} \phi_z(u_i) G_{zz}^z(v, u_i) \right\}
\end{aligned} \tag{45}$$

$$\begin{aligned}
S(t) = & \tilde{\sigma}_{rz}(t) + \sum_{i=1}^N \left\{ \frac{\lambda W_i}{1-s_i} \phi_r(s_i) G_{rz}^r(t, s_i) \right\} + \\
& \sum_{i=1}^N \left\{ \frac{\lambda X_i}{1-u_i} \phi_z(u_i) G_{rz}^z(t, u_i) \right\}.
\end{aligned} \tag{46}$$

Finally, the axial dislocation density B_z is related to the axial displacement of the contact $u_z(r)$ through the following relationship [12]:

$$B_z(r) = -\frac{du_z(r)}{dr}. \tag{47}$$

Thus, $u_z(r)$ can be found by integration:

$$u_z(r) = -\int_d^r B_z(\xi) d\xi. \tag{48}$$

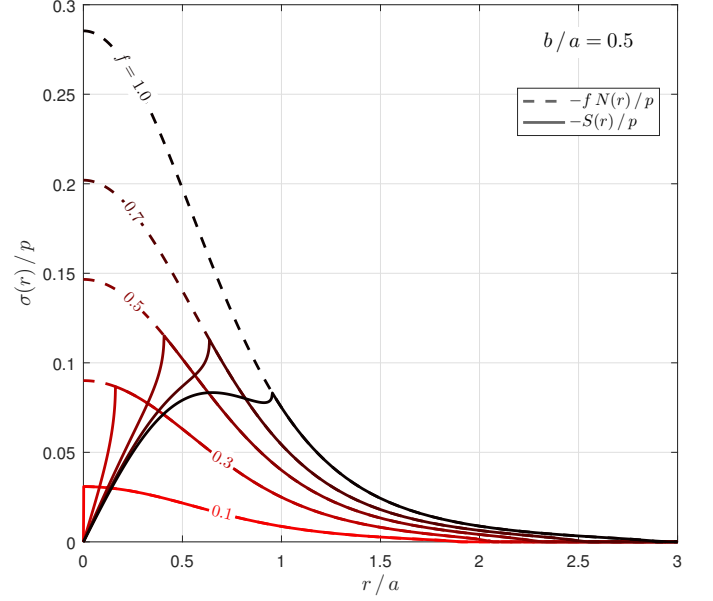


Figure 3: Normalised contact pressure and shear stress in the contact interface for $b/a = 0.5$

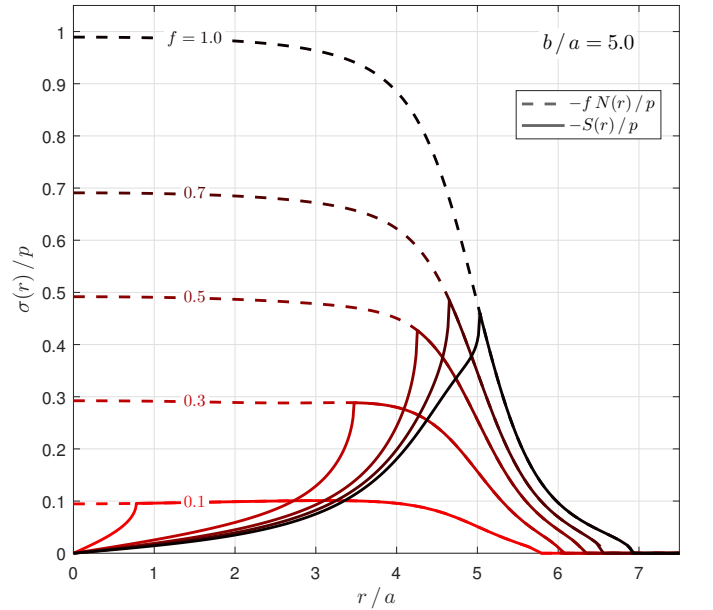


Figure 4: Normalised contact pressure and shear stress in the contact interface for $b/a = 5.0$.

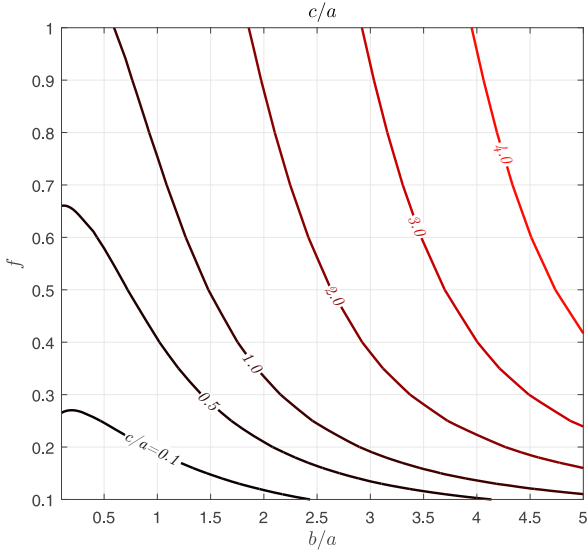


Figure 5: Normalised stick radius c/a .

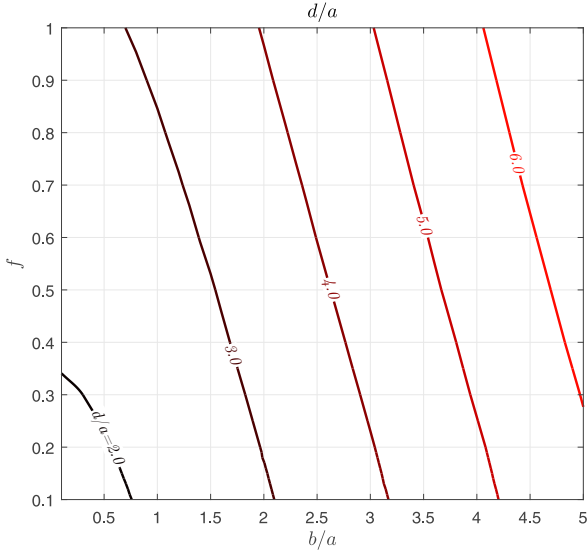


Figure 6: Normalised closure radius d/a .

4. Results

The problem was coded using the numerical processor MATLAB. Due to the semi-infinite nature of the integrals and, consequently, of the mapping functions, the problem is highly non-linear and obtaining a convergent solution is not trivial. First, due to the unknown length dimensions there are additional collocation equations which need to be satisfied and which enable the values of c/a and d/a to be found. In practice, we guess values of the radii to be found and omit the central equations from the $N + 1$ generated for each dislocation. The column vectors of ϕ_i are found. The omitted equations are then evaluated and the lengths needed are adjusted to minimise the residues. Convergence is dependent on obtaining adequate values of quadrature

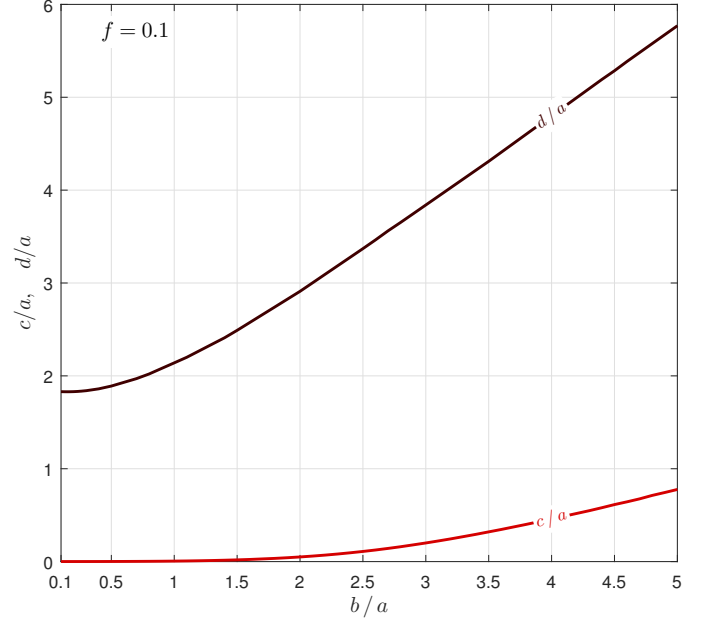


Figure 7: Normalised closure radius d/a and stick radius c/a for $f = 0.1$

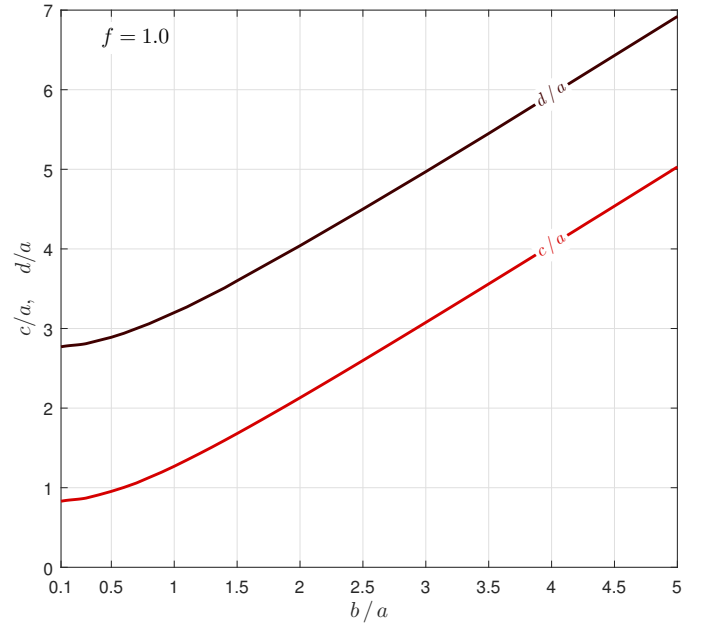


Figure 8: Normalised closure radius d/a and stick radius c/a for $f = 1.0$

points N and the scaling parameter λ . For the present solution, convergence was obtained for $N = 150$ and λ varying between $5a$ and $11a$. Changes in the stresses, displacements, c/a and d/a were negligible when N was increased beyond 150. All results present in this paper are for $\nu = 0.3$.

Figures 3 and 4 show the normalised contact pressure $N(r)$ and shear traction $S(r)$ at the contact interface. As expected, for a fixed coefficient of friction f , the shear stress increases until it reaches $fN(r)$, at which point slip

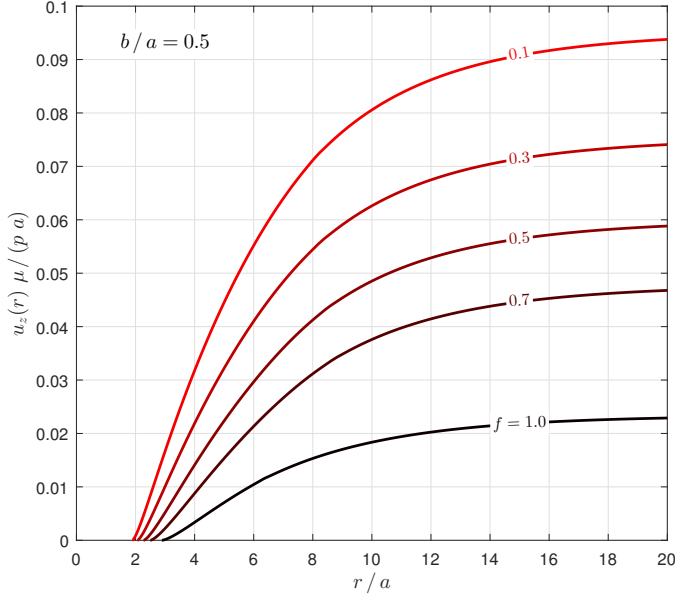


Figure 9: Normalised axial displacement at the contact interface for $b/a = 0.5$.

occurs. From there, the normal and shear tractions fall to zero, where opening occurs. Notice that the tractions are proportional to the magnitude of the applied pressure p . Therefore, the points of slip and opening are independent of p . As a consequence, as soon as an increment of pressure is applied, the contact changes discontinuously from an unloaded configuration to the loaded one [1].

We also note, from eqs. (3) and (4), that the bilateral stresses are independent of the Poisson's ratio. Consequently, this results in the tractions at the contact surface and the points of stick and opening being independent of ν . Therefore, to completely describe the interfacial stresses, only two parameters are needed: f and b/a .

The contours of the normalised points of slip and opening as functions of the coefficient of friction f and the normalised radius of the loaded disk b/a are shown in Figures 5 and 6. It can be noted that as f and b/a increase, c/a and d/a also increase. Figures 7 and 8 show the normalised slip and opening points as a function of b/a for $f = 0.1$ and $f = 1.0$. The region below the c/a curve represents the stick disk, while the region between the d/a and c/a curves shows the slip annulus. For low coefficients of friction ($f = 0.1$ for instance, Figure 7), we notice that as b/a increases the slip annulus becomes larger and accounts for a larger portion of the closed region. For higher f , however ($f = 1.0$, Figure 8), the slip annulus remains approximately of the same size as b/a increases. In this case, the increase in the closed region results in the stick disk becoming larger.

Finally, it is of special interest to look at the contact displacements, especially the axial component, which represents the layer's lifted shape, shown in Figure 9. Away from the origin, the layer is subjected to no shear force across its cross-section, which is similar to a circular plate

under the same loading. As expected, this results in the layer's axial displacement following a logarithmic shape, due to the presence of a non-zero hoop strain. This behaviour was also observed when the bodies were subjected to a normal point force [7].

5. Conclusions

A solution was obtained for the tractions, displacements and geometric parameters for a receding contact between a layer subjected to a disk of pressure and an elastically similar half-space. It was shown that the problem is fully described by two parameters; the coefficient of friction between interfaces and the normalised radius of the loaded disk b/a . For a realistic coefficient of friction, the contact will always be partially open and partially slipping.

In addition, it was shown that the magnitude of pressure p applied to disk does not change the behaviour of the outputs of the problem, since the interfacial tractions are proportional to the applied pressure. The contact's geometric parameters are independent of the pressure which results in the contact changing discontinuously from the unloaded to loaded configuration with the application of an incremental pressure.

With regards to the geometry of the contact, it was noted that the variation of the size of the slip annulus changes considerably with the coefficient of friction. For low f , minimization of the slip annulus size is achieved by reducing the radius of the loaded disk b/a . For high f , however, changes in b/a do not result in significant changes in the slip region's size.

Finally, due to the presence of a non-zero hoop strain, the contact opening presents a logarithmic curvature.

Acknowledgements

J. L. gratefully acknowledges the financial support of Christ Church Oxford, Rolls Royce PLC and Coordenação de Aperfeiçoamento de Pessoal de Nível Superior - CAPES.

References

- [1] J. Dundurs, Properties of elastic bodies in contact, *The Mechanics of the Contact between Deformable bodies* (1975) 54–66.
- [2] T. Chaise, R. Paynter, D. Hills, Contact analysis of a semi-infinite strip pressed onto a half plane by a line force, *International Journal of Mechanical Sciences* 81 (2014) 60–64.
- [3] K. Parel, D. Hills, Frictional receding contact analysis of a layer on a half-plane subjected to semi-infinite surface pressure, *International Journal of Mechanical Sciences* 108 (2016) 137–143.
- [4] L. Keer, J. Dundurs, K. Tsai, Problems involving a receding contact between a layer and a half space, *Journal of Applied Mechanics* 39 (4) (1972) 1115–1120.
- [5] K. Tsai, J. Dundurs, L. Keer, Contact between an elastic layer with a slightly curved bottom and a substrate, *Journal of Applied Mechanics, Transactions ASME* 39 (3) (1972) 821–823.
- [6] K. Tsai, J. Dundurs, L. Keer, Elastic layer pressed against a half space, *Journal of Applied Mechanics* 41 (3) (1974) 703–707.

- [7] J. Lopes, D. Hills, The axisymmetric frictional receding contact of a layer pressed against a half-space by a point force, *International Journal of Solids and Structures* 171 (2019) 47–53.
- [8] J. Lopes, D. Hills, The axisymmetric frictional receding contact of a layer pressed against a half-space by pressure outside a disk, *European Journal of Mechanics-A/Solids* 77 (2019) 103787.
- [9] A. E. H. Love, The stress produced in a semi-infinite solid by pressure on part of the boundary, *Philosophical Transactions of the Royal Society of London. Series A, Containing Papers of a Mathematical or Physical Character* 228 (659-669) (1929) 377–420.
- [10] K.-i. Terazawa, On the elastic equilibrium of a semi-infinite solid under given boundary conditions, *Journal of the College of Science* (1916) 14–24.
- [11] M. T. Hanson, I. W. Puja, Love’s circular patch problem revisited: Closed form solutions for transverse isotropy and shear loading, *Quarterly of applied mathematics* 54 (2) (1996) 359–384.
- [12] D. Hills, P. Kelly, D. Dai, A. Korsunsky, Solution of crack problems: the distributed dislocation technique, Vol. 44 of *Solid Mechanics and Its Applications*, Springer Netherlands, Dordrecht, 2013.
- [13] R. Paynter, D. Hills, The effect of path cut on Somigliana ring dislocations in a half-space, *International Journal of Solids and Structures* 46 (2) (2009) 412–432.
- [14] R. Paynter, D. Hills, A. Korsunsky, The effect of path cut on Somigliana ring dislocation elastic fields, *International Journal of Solids and Structures* 44 (2) (2007) 6653–6677.
- [15] J. Lopes, D. Hills, Ring cracks at the surface of a half-space, *Engineering Fracture Mechanics* 194 (2018) 105–116.
- [16] F. Erdogan, G. D. Gupta, T. Cook, Numerical solution of singular integral equations, in: *Methods of analysis and solutions of crack problems*, 1973, pp. 368–425.
- [17] G. Eason, B. Noble, I. N. Sneddon, On certain integrals of Lipschitz-Hankel type involving products of Bessel functions, *Philosophical Transactions of the Royal Society of London A: Mathematical, Physical and Engineering Sciences* 247 (935) (1955) 529–551.

Appendix A. State of stress induced by circular edge dislocation loops

Appendix A.1. Axial dislocation

Consider a climb axial dislocation loop of radius a put at a depth d and being observed at a position (r, z) in a cylindrical coordinate system, with a Burgers vector component b_z . The stress fields at a position (r, z) are given by

$$\sigma_{iz}^z(r, z) = G_{iz}^z(r, z, d) b_z(a) \quad i = r, z. \quad (\text{A.1})$$

The influence functions $G_{iz}^z(\rho, \zeta, \delta)$ ($i = r, z$) for the glide dislocation in a half-space are given as [13]:

$$G_{zz}^z(\rho, \zeta, \delta) = \frac{2\mu}{a(\kappa + 1)} \left[-J_{1,0;1} + I_{1,0;1} - (\zeta - \delta) J_{1,0;2} - (\zeta + \delta) I_{1,0;2} + 2\zeta\delta I_{1,0;3} \right] \quad (\text{A.2})$$

$$G_{rz}^z(\rho, \zeta, \delta) = \frac{2\mu}{a(\kappa + 1)} \left[-(\zeta - \delta) J_{1,1;2} + (\zeta - \delta) I_{1,1;2} - 2\zeta\delta I_{1,1;3} \right] \quad (\text{A.3})$$

where ρ , ζ and δ are the normalised coordinates, given as

$$\rho = r/a, \quad \zeta = z/a, \quad \delta = d/a, \quad (\text{A.4})$$

μ is the modulus of rigidity and κ is the Kolosov’s constant.

Appendix A.2. Radial dislocation

The radial dislocation is not of Volterra kind and, thus, is path-cut dependent. In this paper, an ‘outside disk’ path cut is used [13]. This path cut can be formed by inserting a disk of material at a depth $z = d$, from $r = a$ to $r = \infty$, displacing the material by the same amount b_r (thickness of the disk). The stress fields at a position (r, z) are given by

$$\sigma_{iz}^r(r, z) = G_{iz}^r(r, z, d) b_r(a) \quad i = r, z. \quad (\text{A.5})$$

The influence functions $G_{iz}^r(\rho, \zeta, \delta)$ ($i = r, z$) for the glide dislocation in a half-space are given as [13]:

$$G_{zz}^r(\rho, \zeta, \delta) = \frac{2\mu}{a(\kappa + 1)} \left[-(\zeta - \delta) J_{0,0;2} + (\zeta - \delta) I_{0,0;2} + 2\zeta\delta I_{0,0;3} \right] \quad (\text{A.6})$$

$$G_{rz}^r(\rho, \zeta, \delta) = \frac{2\mu}{a(\kappa + 1)} \left[J_{0,1;1} - I_{0,1;1} - (\zeta - \delta) J_{0,1;2} + (\zeta + \delta) I_{0,1;2} - 2\zeta\delta I_{0,1;3} \right] \quad (\text{A.7})$$

Appendix A.3. Lipschitz-Hankel integrals

In the influence functions, the terms $J_{n,p;q}$ and $I_{n,p;q}$ represent Lipschitz-Hankel integrals. The standard definition for these functions is as an integral of the product of Bessel functions ($J_i(\cdot)$), an exponential term and a power term. Using normalised coordinate variables, it is given as [17]

$$P_{\mu,\nu;\lambda}(\rho, \zeta) = \int_0^\infty J_\mu(t) J_\nu(\rho t) e^{-\zeta t} t^\lambda dt. \quad (\text{A.8})$$

In the kernels, the follow definition is applied:

$$J_{n,p;q} = P_{n,p;q}(\rho, \zeta - \delta) \quad (\text{A.9})$$

$$I_{n,p;q} = P_{n,p;q}(\rho, -\zeta - \delta) \quad (\text{A.10})$$

The Lipschitz-Hankel integrals needed in the kernels are given by Paynter et al. [14, 13].